Journal of Sound and Vibration (2000) **229**(4), 755–773
doi:10.1006/jsvi.1999.2527, available online at http://www.idealibrary.com on IDEAL®

FREE VIBRATION AND BUCKLING OF IN-PLANE LOADED PLATES WITH ROTATIONAL ELASTIC EDGE SUPPORT

D. J. GORMAN

Department of Mechanical Engineering, University of Ottawa, 770 King Edward Avenue, Ottawa, Canada, K1N 6N5

(*Received* 19 *March* 1999)

The superposition method is employed to obtain buckling loads and free vibration frequencies for a family of elastically supported rectangular plates subjected to one-directional uniform in-plane loading. Two edges running in the direction of the in-plane loading are free. Lateral displacement is forbidden along the other two edges which are given uniform elastic rotational support. Accurate buckling loads are tabulated for a fairly broad range of plate geometries and edge support stiffnesses. Computed free vibration eigenvalues are also tabulated for square plates with typical in-plane loading and a range of stiffnesses in the edge supports.

1. INTRODUCTION

A number of publications have appeared in the technical literature in which the free vibration and buckling of rectangular plates subjected to uniform in-plane loading have been analyzed. A fairly extensive review of literature related to both of these phenomena has been provided by Michelussi [1]. While the buckling of such plates has traditionally been studied under the subject of plate static behaviour, it is known that plate buckling can also be readily studied in conjunction with plate-free vibration behaviour. This is possible because it is known that we can treat the buckling phenomenon as one associated with a limiting case of free vibration. This limiting case is arrived at when the in-plane compressive loading is increased to a level where the plate first mode free vibration frequency takes on a value of zero. The in-plane loading associated with this zero frequency is, in fact, the buckling load.

A number of fairly recent publications have appeared in the literature in which the two phenomenon of buckling and free vibration have been studied by means of essentially the same analysis [1–3]. These studies have been conducted for plates with combinations of classical edge conditions. All have been conducted by means of the method of superposition.

It is well known that classical boundary conditions as formulated mathematically represent conditions of idealized edge support. In actual fact, there will be some elasticity in the plate edge restraints. This elasticity may enter the boundaries unintentionally or, it may be there as a result of rational design.

0022-460X/00/040755 + 19 $35.00/0

In this paper, we consider the free vibration and buckling of thin rectangular plates with two opposite free edges and uniform in-plane loading running parallel to these free edges. Along the opposite edges where in-plane loading is applied, plate lateral displacement is forbidden. Plate rotation along these edges, however, is not forbidden but, due to rotational elastic restraint, is opposed by bending moments proportional to the degree of edge rotation. It will already be apparent that two natural limits for this uniform elastic support exit. When the elastic efficient associated with this edge support approaches infinity, we approach the classical "clamped edge" condition. When this same coefficient approaches zero we approach "simple support" conditions.

The analysis of this family of plate problems is conducted by means of the method of superposition. Free vibration and buckling results are computed for the case where elastic restraint acts along one of the in-plane loaded edges, only, the other being given essentially simple support. Similar studies are also conducted for the case where elastic restraint acts simultaneously along each of these opposite edges. It will be seen that the superposition method provides a highly accurate and straightforward solution to each family of problems.

2. MATHEMATICAL PROCEDURE

We begin by analyzing the rectangular plate with elastic rotational restraint along one edge, only. It is found advantageous to conduct this analysis in two separate steps. First, we develop the analysis for the situation where the edge, to be ultimately given rotational elastic support, has clamped edge conditions imposed. It will then be shown that with minor modifications to the eigenvalue matrix developed for this initial problem, we arrive at the appropriate eigenvalue matrix to be utilized for analysis of the plate with elastic restraint along its boundary.

2.1. DEVELOPMENT OF BUILDING BLOCK SOLUTIONS

Analysis for free vibration and buckling of the above plate with clamped edge conditions imposed is achieved by superposition of the three forced vibration problems (building blocks) represented in Figure 1. All building blocks are subjected to one-directional uniform in-plane compressive loading as indicated in the figure.

The first building block is given simple support along the two in-plane loaded edges. The edge, $\eta = 0$, is given slip shear support, indicated by two small adjacent circles. Vertical edge reaction along this edge, as well as slope taken normal to the edge, is everywhere zero. The edge, $\eta = 1$, is free of vertical edge reaction but is driven by an enforced distributed harmonic edge rotation of circular frequency ω. We begin by obtaining the solution for the response of this building block to the harmonic excitation.

The principal reference for the work reported here is that of Michelussi [1]. In fact, the first step in the present analysis related to imposed clamped edge conditions as discussed above, follows essentially the analysis discussed by

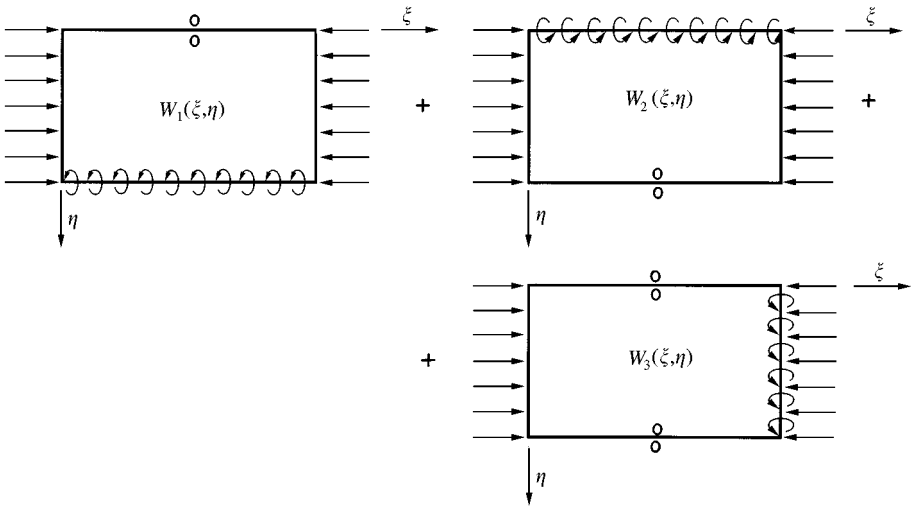

Figure 1. Schematic representation of building blocks employed in analyzing rectangular plate with one elastically supported edge.

Michelussi. For this reason only a brief description of the first step in the analysis will be given for the sake of completeness.

The governing differential equation in dimensionless form becomes [1],

$$\frac{\partial^4 W(\xi,\eta)}{\partial\eta^4} + 2\phi^2 \frac{\partial^4 W(\xi,\eta)}{\partial\eta^2 \partial\xi^2} + \phi^4 \frac{\partial^4 W(\xi,\eta)}{\partial\xi^4} + P_\xi \phi^2 \frac{\partial^2 W(\xi,\eta)}{\partial\xi^2} - \lambda^4 \phi^4 W(\xi,\eta) = 0, \tag{1}$$

where the dimensionless in-plane load parameters $P_\xi = P_x b/D$. While P_ξ represents a positive compressive load, negative values for P_ξ represent tensile loads.

Expressions for dimensionless bending moments and vertical edge reactions for the present problem differ from those related to problems without in-plane loading only in that dimensionless vertical edge reactions along the edges, $\xi = 0$ and 1, are expressed as

$$\frac{Va^2}{D} = -\left\{\frac{\partial^3 W(\xi,\eta)}{\partial\xi^3} + \frac{\nu^*}{\phi^2}\frac{\partial^3 W(\xi,\eta)}{\partial\xi\partial\eta^2} + \frac{P_\xi}{\phi^2}\frac{\partial W(\xi,\eta)}{\partial\xi}\right\}. \tag{2}$$

Focussing on the first building block, the amplitude of the enforced edge rotation is expressed as

$$Y'(\eta)|_{\eta=1} \sum_{m=1,2}^{\infty} E_m \sin m\pi\xi, \tag{3}$$

where primes indicate differentiation with respect to η.

The solution for plate lateral displacement associated with response of the building block is expressed as

$$W(\xi,\eta) = \sum_{m=1,2}^{\infty} Y_m(\eta) \sin m\pi\xi. \tag{4}$$

Substituting equation (4) into equation (1), an ordinary homogeneous differential equation involving the function $Y_m(\eta)$ is obtained as

$$Y_m''''(\eta) - 2\phi^2 \delta_m Y_m''(\eta) + \phi^4 \Delta_m Y_m(\eta) = 0, \tag{5}$$

where

$$\delta_m = (m\pi)^2 \quad \text{and} \quad \Delta_m = (m\pi)^4 - \lambda^4 - P_\xi (m\pi/\phi)^2.$$

The four roots of the characteristic equation related to equation (5) are given as

$$r = \pm \phi \sqrt{\delta_m \pm \sqrt{\delta_m^2 - \Delta_m}}. \tag{6}$$

We note that δ_m will always be greater than zero. It follows therefore that three distinct solutions of equation (5) are possible. We will treat these three distinct cases as follows. Case 1: $\delta_m^2 < \Delta_m$. Case 2: $\delta_m^2 > \Delta_m$, $\Delta_m < 0{\cdot}0$. Case 3: $\delta_m^2 > \Delta_m$, $\Delta_m > 0{\cdot}0$.

The solutions associated with these cases are

Case 1:

$$Y_m(\eta) = A_m \sinh(\beta_m \eta) \sin(\gamma_m \eta) + B_m \sinh(\beta_m \eta) \cos(\gamma_m \eta) + C_m \cosh(\beta_m \eta) \sin(\gamma_m \eta) + D_m \cosh(\beta_m \eta) \cos(\gamma_m \eta), \tag{7}$$

where

$$\beta_m = \phi \sqrt{\frac{\sqrt{\Delta_m} + \delta_m}{2}} \quad \text{and} \quad \gamma_m = \phi \sqrt{\frac{\sqrt{\Delta_m} - \delta_m}{2}}.$$

Case 2:

$$Y_m(\eta) = A_m \sinh(\beta_m \eta) + B_m \cosh(\beta_m \eta) + C_m \sin(\gamma_m \eta) + D_m \cos(\gamma_m \eta), \tag{8}$$

where

$$\beta_m = \phi \sqrt{\sqrt{\delta_m^2 - \Delta_m} + \delta_m} \quad \text{and} \quad \gamma_m = \phi \sqrt{\sqrt{\delta_m^2 - \Delta_m} - \delta_m}.$$

Case 3;

$$Y_m(\eta) = A_m \sinh(\beta_m \eta) + B_m \cosh(\beta_m \eta) + C_m \sinh(\gamma_m \eta) + D_m \cosh(\gamma_m \eta), \tag{9}$$

where

$$\beta_m = \phi \sqrt{\delta_m + \sqrt{\delta_m^2 - \Delta_m}} \quad \text{and} \quad \gamma_m = \phi \sqrt{\delta_m - \sqrt{\delta_m^2 - \Delta_m}}.$$

The quantities A_m, B_m, etc., above are to be evaluated according to the prescribed boundary conditions.

Returning to the first building block it will be obvious that all antisymmetric terms in the solutions must be deleted.

The remaining two unknowns are evaluated by means of the two boundary conditions which must be enforced along the driven edge. They are expressed as

$$\frac{\partial^3 W(\xi,\eta)}{\partial \xi^3} + \nu^+ \phi^2 \frac{\partial^3 W(\xi,\eta)}{\partial \eta \, \partial \xi^2}\bigg|_{\eta=1} = 0 \tag{10}$$

and

$$Y'_m(\eta)|_{\eta=1} = E_m. \tag{11}$$

Enforcing these two boundary conditions we obtain the following.

Case 1:

$$Y_m(\eta) = E_m\{\theta_{11m}\sinh\beta_m\eta\sin\gamma_m\eta + \theta_{14m}\cosh\beta_m\eta\cos\gamma_m\eta\}, \tag{12}$$

where

$$X1 = \beta_m(\beta_m^2 - 3\gamma_m^2)\sinh\beta_m\cos\gamma_m,\ X2 = \gamma_m(3\beta_m^2 - \gamma_m^2)\cosh\beta_m\sin\gamma_m,$$

$$X3 = \beta_m\sinh\beta_m\cos\gamma_m,\ X4 = \gamma_m\cosh\beta_m\sin\gamma_m, \tag{13}$$

$$\theta_{11m} = \frac{-\{X1 - X2 - (2-\nu)(m\pi\phi)^2(-X3 + X4)\}}{2\beta_m\gamma_m(\beta_m^2 + \gamma_m^2)(\sinh^2\beta_m + \sin^2\gamma_m)}$$

and

$$X1 = (2-\nu)(m\pi\phi)^2\beta_m\cosh\beta_m\sin\gamma_m,\ X2 = (2-\nu)(m\pi\phi)^2\gamma_m\sinh\beta_m\cos\gamma_m,$$

$$X3 = \beta_m(\beta_m^2 - 3\gamma_m^2)\cosh\beta_m\sin\gamma_m,\ X4 = \gamma_m(3\beta_m^2 - \gamma_m^2)\sinh\beta_m\cos\gamma_m,$$

$$\theta_{14m} = \frac{-\{X1 + X2 - X3 - X4]}{2\beta_m\gamma_m(\beta_m^2 + \gamma_m^2)(\sinh^2\beta_m + \sin^2\gamma_m)}. \tag{14}$$

Case 2:

$$Y_m(\eta) = E_m\{\theta_{22m}\cosh\beta_m\eta + \theta_{24m}\cos\gamma_m\eta\}, \tag{15}$$

where

$$\theta_{22m} = \left[\frac{\gamma_m^2 + (2-\nu)(m\pi\phi)^2}{\beta_m(\beta_m^2 + \gamma_m^2)\sinh(\beta_m)}\right],\quad \theta_{24m} = \left[\frac{\beta_m^2 - (2-\nu)(m\pi\phi)^2}{\gamma_m(\beta_m^2 + \gamma_m^2)\sin(\gamma_m)}\right]. \tag{16, 17}$$

Case 3

$$Y_m(\eta) = E_m\{\theta_{33m}\cosh\beta_m\eta + \theta_{34m}\cosh\gamma_m\eta\}, \tag{18}$$

where

$$\theta_{33m} = \left[\frac{(2-\nu)(m\pi\phi)^2 - \gamma_m^2}{\beta_m(\beta_m^2 - \gamma_m^2)\sinh(\beta_m)}\right],\quad \theta_{34m} = \left[\frac{\beta_m^2 - (2-\nu)(m\pi\phi)^2}{\gamma_m(\beta_m^2 - \gamma_m^2)\sinh(\gamma_m)}\right]. \tag{19, 20}$$

We thus have available the response of the first building block for all possible geometries, driving frequencies, and in-plane loading.

Attention is next focussed on the second building block. It differs from the first, only in that edge conditions along the boundaries, $\eta = 0$ and 1, are interchanged.

A solution is extracted from that of the first building block through replacing η, with the quantity $(1-\eta)$. Also, in view of sign conventions, a negative sign must preceede the solution for the second building block obtained in this manner.

Finally, we turn to the third building block of Figure 1. Simple support is imposed along the edge, $\xi = 0$, while the other two non-driven edges are given slip-shear support. Lateral displacement is forbidden at the remaining edge which is driven by a distributed harmonic bending moment. In view of the in-plane forces the solution for this building block cannot be obtained, through a transformation of axis, from any solution of the type already discussed. Rather we must start from first principles.

The amplitude of the driving moment is expressed as

$$\left.\frac{Ma}{D}\right|_{\xi=1} = \sum_{n=0,1,2}^{\infty} E_n \cos n\pi\eta. \tag{21}$$

Solution for plate lateral displacement is expressed as

$$W(\xi,\eta) = \sum_{n=0,1,2}^{\infty} Y_n(\xi)\cos n\pi\eta. \tag{22}$$

Substituting equation (22) into equation (1) it is found that the ordinary differential equation governing the functions $Y_n(\xi)$ becomes

$$Y_n''''(\xi) - \frac{2\delta_n}{\phi^2}\, Y_n''(\xi) + \frac{\Delta_n}{\phi^4}\, Y_n(\xi) = 0, \tag{23}$$

where

$$\delta_n = (n\pi)^2 - \frac{P_\xi}{2} \quad \text{and} \quad \Delta_n = (n\pi)^4 - \lambda^4\phi^4.$$

The roots of the characteristic equation associated with equation (23) are

$$r = \pm\frac{1}{\phi}\sqrt{\delta_n \pm \sqrt{\delta_n^2 - \Delta_n}}\,. \tag{24}$$

It is found that both δ_n and Δ_n may now each take on positive or negative values. Four distinct forms of solution are thus possible and we again designate these four distinct cases as follows:

Case 1: $\delta_n^2 < \Delta_n$.
Case 2: $\delta_n^2 > \Delta_n,\ \Delta_n < 0{\cdot}0$.
Case 3: $\delta_n^2 > \Delta_n,\ \Delta_n > 0{\cdot}0,\ \delta_n > 0{\cdot}0$.
Case 4: $\delta_n^2 > \Delta_n,\ \Delta_n > 0{\cdot}0,\ \delta_n < 0{\cdot}0$.

Solutions associated with these cases are as follows.

Case 1:

$$\begin{aligned} Y_n(\xi) = {} & A_n \sinh(\beta_n\xi)\sin(\gamma_n\xi) + B_n \sinh(\beta_n\xi)\cos(\gamma_n\xi) \\ & + C_n \cosh(\beta_n\xi)\sin(\gamma_n\xi) + D_n \cosh(\beta_n\xi)\cos(\gamma_n\xi)\,, \end{aligned} \tag{25}$$

where

$$\beta_n = \frac{1}{\phi}\sqrt{\frac{\sqrt{\Delta_n} + \delta_n}{2}} \quad \text{and} \quad \gamma_n = \frac{1}{\phi}\sqrt{\frac{\sqrt{\Delta_n} + \delta_n}{2}}.$$

Case 2:

$$Y_n(\xi) = A_n \sinh(\beta_n \xi) + B_n \cosh(\beta_n \xi) + C_n \sin(\gamma_n \xi) + D_n \cos(\gamma_n \xi), \tag{26}$$

where

$$\beta_n = \frac{1}{\phi}\sqrt{\sqrt{\delta_n^2 - \Delta_n} + \delta_n} \quad \text{and} \quad \gamma_n = \frac{1}{\phi}\sqrt{\sqrt{\delta_n^2 - \Delta_n} - \delta_n}.$$

Case 3:

$$Y_n(\xi) = A_n \sinh(\beta_n \xi) + B_n \cosh(\beta_n \xi) + C_n \sinh(\gamma_n \xi) + D_n \cosh(\gamma_n \xi), \tag{27}$$

where

$$\beta_n = \frac{1}{\phi}\sqrt{\delta_n + \sqrt{\delta_n^2 - \Delta_n}} \quad \text{and} \quad \gamma_n = \frac{1}{\phi}\sqrt{\delta_n - \sqrt{\delta_n^2 - \Delta_n}}.$$

Case 4:

$$Y_n(\xi) = A_n \sin(\beta_n \xi) + B_n \cos(\beta_n \xi) + C_n \sin(\gamma_n \xi) + D_n \cos(\gamma_n \xi), \tag{28}$$

where

$$\beta_n = \frac{1}{\phi}\sqrt{-\delta_n - \sqrt{\delta_n^2 - \Delta_n}} \quad \text{and} \quad \gamma_n = \frac{1}{\phi}\sqrt{-\delta_n + \sqrt{\delta_n^2 - \Delta_n}}.$$

It will be obvious that only the antisymmetric terms can be retained in the above solutions. The remaining constants are evaluated by means of boundary conditions imposed at the driven edge and formulated as

$$Y_n(\xi)|_{\xi=1} = 0, \quad \text{and} \quad Y_n''(\xi)|_{\xi=1} = -E_n. \tag{29, 30}$$

Enforcing these conditions we obtain the solutions as follows.

Case 1:

$$Y_n(\xi) = E_n\{\theta_{11n} \sinh \beta_n \xi \cos \gamma_n \xi + \theta_{15n} \cosh \beta_n \xi \sin \gamma_n \xi\}, \tag{31}$$

where

$$\theta_{11n} = \left[\frac{-\cosh(\beta_n)\sin(\gamma_n)}{2\beta_n\gamma_n(\cos^2(\gamma_n) - \cosh^2(\beta_n))}\right], \quad \theta_{15n} = -\left[\frac{-\sinh(\beta_n)\cos(\gamma_n)}{2\beta_n\gamma_n(\cos^2(\gamma_n) - \cosh^2(\beta_n))}\right]. \tag{32, 33}$$

Case 2:

$$Y_n(\xi) = E_n\{\theta_{22n}\sinh\beta_n\xi + \theta_{25n}\sinh\gamma_n\xi\}, \tag{34}$$

where

$$\theta_{22n} = \frac{-1{\cdot}0}{(\beta_n^2+\gamma_n^2)\sinh\beta_n}, \quad \theta_{25n} = \frac{1{\cdot}0}{(\beta_n^2+\gamma_n^2)\sin\gamma_n}. \tag{35, 36}$$

Case 3:

$$Y_n(\xi) = E_n\{\theta_{33n}\sinh\beta_n\xi + \theta_{35n}\sinh\gamma_n\xi\}, \tag{37}$$

where

$$\theta_{33n} = \frac{-1{\cdot}0}{(\beta_n^2-\gamma_n^2)\sinh\beta_n}, \quad \theta_{35n} = \frac{1{\cdot}0}{(\beta_n^2-\gamma_n^2)\sinh\gamma_n}. \tag{38, 39}$$

Case 4:

$$Y_n(\xi) = E_n\{\theta_{44n}\sin\beta_n\xi + \theta_{45n}\sin\gamma_n\xi\}, \tag{40}$$

where

$$\theta_{44n} = \frac{-1{\cdot}0}{(\gamma_n^2-\beta_n^2)\sin\beta_n}, \quad \theta_{45n} = \frac{1{\cdot}0}{(\gamma_n^2-\beta_n^2)\sin\gamma_n}. \tag{41, 42}$$

2.2 DEVELOPMENT OF THE EIGENVALUE MATRIX

Generation of the eigenvalue matrix follows established procedures. The net contributions of all three building blocks to bending moments along the edges, $\eta = 1$ and 0, are expanded in sine series of K terms, and the net coefficients in each of these series are set equal to zero. This gives rise to a set of $2K$ homogeneous algebraic equations relating the $3K$ unknown driving coefficients. A further set of homogeneous algebraic equations is obtained through expanding the net contributions of the three building blocks toward the slope along the edge, $\xi = 1$, in a cosine series. The eigenvalue matrix is composed of the coefficient matrix for these sets of homogeneous equations. A schematic representation of the eigenvalue matrix is provided in Figure 2.

2.3. MODIFICATION OF EIGENVALUE MATRIX TO INCLUDE ELASTIC EDGE EFFECTS

Let us consider now the boundary condition to be satisfied along the edge, $\xi = 1$, when this edge is given uniform rotational elastic support. In dimensional form the boundary condition is expressed as

$$M = k\frac{\partial w}{\partial x}, \tag{43}$$

where k is the basic rotational elastic stiffness.

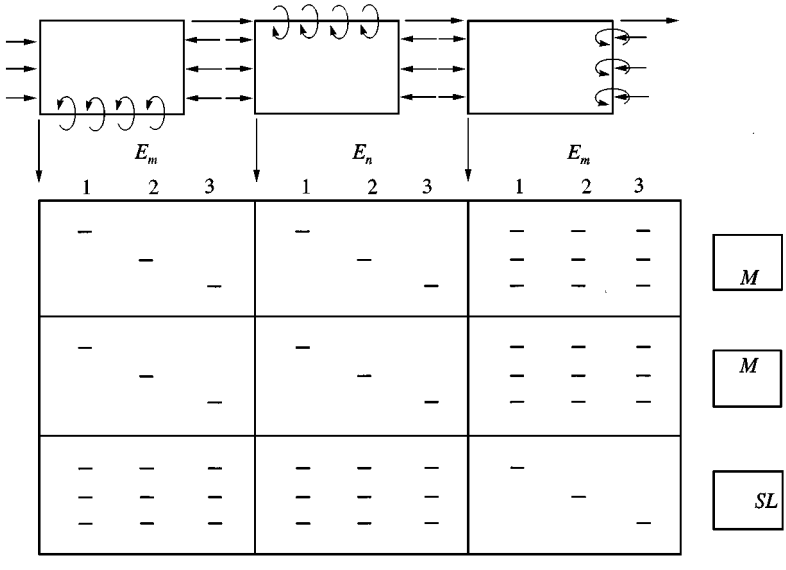

Figure 2. Schematic representation of eigenvalue matrix utilized in analyzing behaviour of rectangular plate with one elastically supported edge.

The above equation may be written in dimensionless homogeneous form as

$$\frac{Ma}{D} - K_R \frac{\partial W}{\partial \xi} = 0, \tag{44}$$

where $K_R = ka/D$ is the dimensionless rotational elastic stiffness.

Returning now to the matrix of Figure 2 it is seen that the effects of this rotational elastic edge support may be incorporated into the matrix by performing the following two simple operations.

(1) Multiply each element in the lower three segments of the matrix by the quantity K_R.
(2) Subtract the quantity, 1·0, from each element along the diagonal of the lower right-hand segment of the matrix.

Before discussing the computation and presentation of results, it is appropriate to briefly describe the modifications to the matrix of Figure 2 which will be necessary when we wish to examine the current plate problem with rotational elastic support also provided along the edge, $\xi = 0$.

It will be obvious that we must now add a fourth building block to those of Figure 1, i.e., a building block which differs from the third, only in that it is driven by a distributed harmonic bending moment along the edge, $\xi = 0$. The solution for the response of this building block will, of course, be easily extracted from that of the third building block. There will now be $4K$ unknown driving coefficients; however, we will have four sets of homogeneous equations available, based on the prescribed boundary conditions. The eigenvalue matrix of Figure 2 will now be composed of 16 segments, four across and four down. Post-modifications required

to incorporate the effects of rotational elasticity into the matrix will be almost identical to those described above.

All elements in the third row of segments will again be multiplied by the dimensionless stiffness parameter K_{R2}, while all elements in the final row of segments will be multiplied by the factor, K_{R4}. Subscripts 2 and 4, refer to the edges, $\xi = 1$ and 0, respectively. Again, the quantity 1·0 will be subtracted from diagonal elements of the third segment of the third row; however it will be added to the diagonal elements of the lower right-hand segment of the matrix. Addition is required here, rather than subtraction, because equation (44) when applied to the edge, $\xi = 0$, will have a positive sign preceding the last term.

There is one further aspect to the generation of the eigenvalue matrix which should be elaborated upon here, particularly in that it is not considered by Michelussi [1]. Returning to equation (23) it is seen that with the quantity, $n\pi$ and λ^2 equal to zero (during buckling studies) the quantity γ_n of equation (28) will also be equal to zero. This would result in the quantity θ_{45n} of equation (42) taking on a value of infinity.

This difficulty can be obviated by recognizing that with the quantity Δ_n equal to zero the final term of equation (23) vanishes. The equation can therefore be written as

$$Y_n''''(\xi) + \alpha^2 Y_n''(\xi) = 0, \tag{45}$$

where

$$\alpha^2 = P_\xi/\phi^2.$$

The solution to equation (45) is written as

$$Y_n(\xi) = A\sin\alpha\xi + B\cos\alpha\xi + C\xi + D. \tag{46}$$

Enforcing the boundary conditions at $\xi = 0$ and 1, the solution becomes

$$Y_n(\xi) = \frac{E_n}{\alpha^2 \sin\alpha}\{\sin\alpha\xi - \xi\sin\alpha\}. \tag{47}$$

Utilizing the above equation one can now enter the contributions associated with equation (40) into the eigenvalue matrix when "n" equals zero.

3. COMPUTATION AND PRESENTATION OF RESULTS

We are now in a position to compute buckling loads and free vibration frequencies and mode shapes for the elastically supported plates, with uniform in-plane loading, under consideration. As will be seen shortly, it is found advantageous to begin by computing buckling loads.

Buckling loads are computed by proceeding as follows. The eigenvalue, λ^2, is set equal to zero and a trial compressive buckling load, P_ξ, is selected. The determinant of the associated eigenvalue matrix is computed and stored. The trial buckling load is then augmented slightly, and the process is repeated until the lowest value of P_ξ is established for which the determinant of the matrix vanishes. This value of P_ξ is the buckling load for the plate under study.

Free vibration eigenvalues are computed in a similar fashion except, of course, now the in-plane loading is fixed and we search for values of the parameter λ^2 which cause the determinant of the associated matrix to vanish. The in-plane loading imposed during free vibration studies must, of course, be less than the plate buckling load. It is customary to impose fixed in-plane loading which is some fraction (less than 100%) of the actual plate buckling load. For this reason, the practice of computing buckling loads before computing free vibration eigenvalues is often followed. In either case, whether conducting buckling or free vibration studies, once the buckling loads or eigenvalues are established, associated mode shapes are determined by setting one of the non-zero driving coefficients equal to unity and solving the resulting set of non-homogeneous equations for the others. It will be recalled that for plates, mode shapes associated with buckling may not be the same as first mode free vibration mode shapes. The reader will now appreciate that the analysis as described here permits studies of plates with elastic support at one, or both edges of the plate. One may use the more general computer program for all studies and simply focus on the smaller portion of the eigenvalue matrix when one edge is free of elastic support.

3.1. RESULTS OF BUCKLING STUDIES

All buckling loads reported here, as well as free vibration eigenvalues, have been computed with building block solutions based on 11 term expansions. Convergence studies indicated that accuracy up to four significant digits in computed results could be obtained by means of seven term solutions. Nevertheless, 11 terms were utilized here and all results are tabulated with four-digit accuracy.

It will be recalled that natural limits for both buckling loads and free vibration eigenvalues exist, when the rotational elastic coefficients and allowed to take on limits of zero and infinity. The matrix as described above can be utilized to handle the extreme case, when the elastic coefficient approaches infinity, i.e., the clamped edge condition, by simply deleting the matrix post-generation modifications as described. All data obtained for these two extreme cases have been compared with the classical edge condition results of Michelussi [1]. Excellent agreement has been found between the two limiting sets of data. This comparison acts as a partial verification for the present analysis.

In the data to be presented it will be understood that results for only a very limited set of problems can be tabulated or plotted. This is because of the numerous parameters involved, in-plane load intensities, stiffness coefficients, plate aspect ratios, etc. The main objectives of the plotted curves will be to provide insight into how the buckling-vibratory systems can be expected to behave with varying elastic stiffness. Tabulated results will provide digital data against which other research workers can compare their findings for the purposes of verification.

A plot of bucklings load versus edge elastic stiffness coefficient is presented in Figure 3 for a square plate with elastic support along one edge only. The buckling curve begins at the correct lower limit and rises to eventually approach the known upper limit. It is observed, as might be expected, that the buckling load is much more sensitive to edge stiffness coefficient in the lower range of this parameter, K_{R2}.

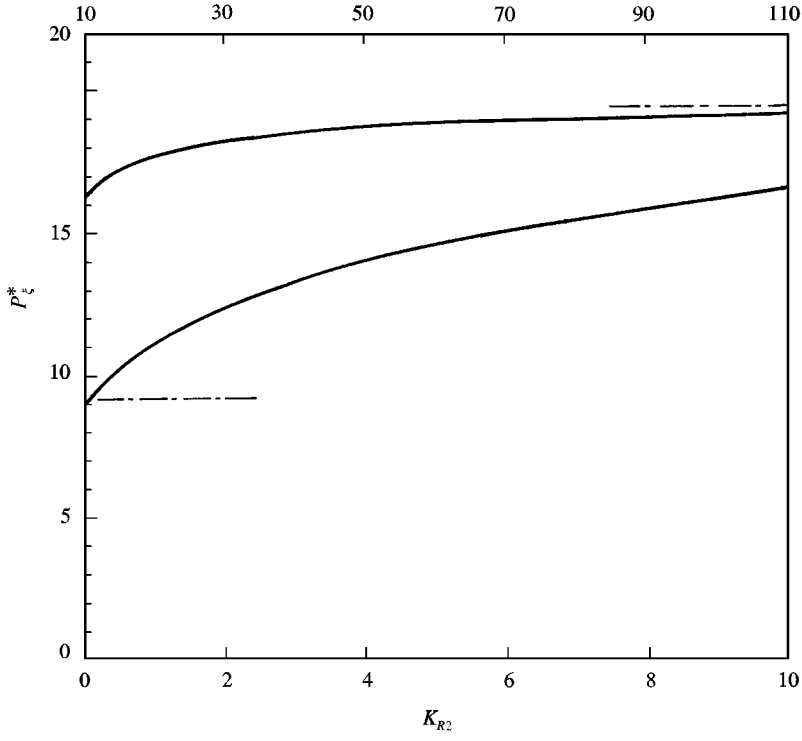

Figure 3. Buckling load versus rotational elastic edge stiffness for square plate with elastic support along one edge, only.

A similar buckling curve is plotted in Figure 4 for a square plate with equal elastic stiffnesses applied at opposite edges. The curve begins, of course, at the same loading value as that of the previous figure. Again, it rises relatively rapidly at first and finally approaches the known buckling load for a plate with the opposite edges clamped.

Buckling loads for plates with elastic support along one edge only, and various combinations of elastic stiffness coefficient and plate aspect ratio, are tabulated in Tables 1–5. In Tables 6–10, data are presented over a similar range of the above parameters for plates with equal elastic support along the opposite edges. Selection of discrete values of dimensionless stiffness parameter utilized in these tables was based on the curves of Figures 3 and 4. An attempt has been made to choose intervals in the stiffness parameter which give rise to approximately equal intervals in the associated buckling loads.

A plot of data for the above tables reveals that tabulated values lie along continuous curves running between the lower and upper limits.

3.2. RESULTS OF FREE VIBRATION EIGENVALUE STUDIES

A plot of first mode eigenvalue versus stiffness coefficient for a square plate subjected to an in-plane loading is presented in Figure 5. Here the plate is given

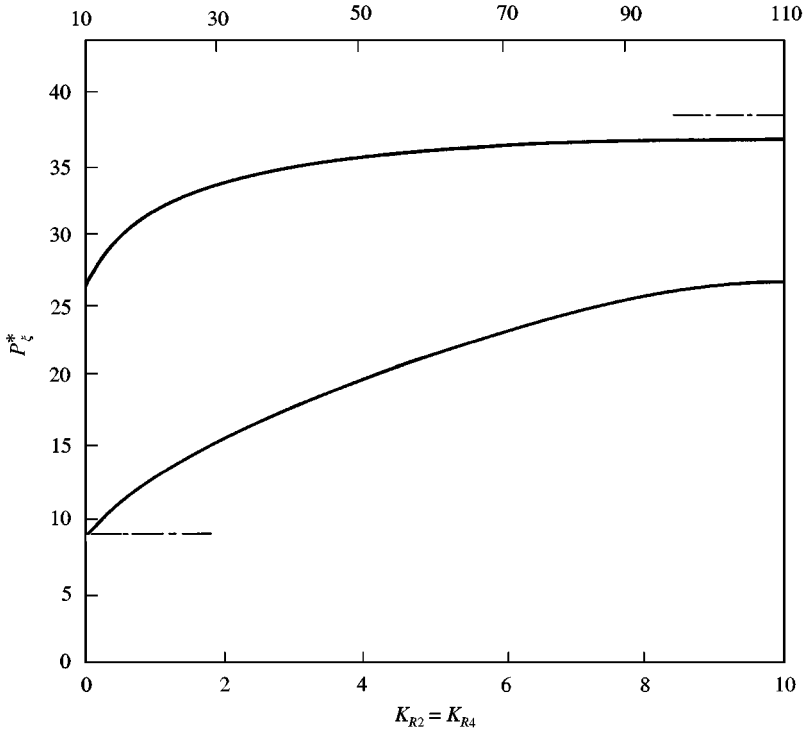

Figure 4. Buckling load versus rotational elastic stiffness for square plate. Equal elastic support acts along opposite edges.

TABLE 1

Buckling loads for plate with elastic support along one edge ($\phi = 1{\cdot}0$)

K_{R2}	P^*	K_{R2}	P^*	K_{R2}	P^*	K_{R2}	P^*
0·0	9·276	1·6	11·82	6·0	15·12	24·0	17·94
0·4	10·03	2·0	12·29	10·0	16·39	30·0	18·21
0·8	10·70	3·0	13·27	14·0	17·09	50·0	18·66
1·2	11·29	4·0	14·03	18·0	17·52	∞	19·40

TABLE 2

Buckling loads for plate with elastic support along one edge ($\phi = 1{\cdot}5$)

K_{R2}	P^*	K_{R2}	P^*	K_{R2}	P^*	K_{R2}	P^*
0·0	21·23	1·6	26·95	6·0	34·43	24·0	40·83
0·4	22·93	2·0	28·02	10·0	37·30	30·0	41·43
0·8	24·43	3·0	30·23	14·0	38·89	50·0	42·46
1·2	25·76	4·0	31·95	18·0	39·88	∞	44·14

TABLE 3

Buckling loads for plate with elastic support along one edge ($\phi = 2{\cdot}5$)

K_{R2}	P^*	K_{R2}	P^*	K_{R2}	P^*	K_{R2}	P^*
0·0	59·93	1·6	75·83	6·0	96·68	24·0	114·6
0·4	64·64	2·0	78·80	10·0	104·7	30·0	116·3
0·8	68·82	3·0	84·96	14·0	109·1	50·0	119·1
1·2	72·52	4·0	89·76	18·0	111·9	∞	123·9

TABLE 4

Buckling loads for plate with elastic support along one edge ($\phi = 1/1{\cdot}5$)

K_{R2}	P^*	K_{R2}	P^*	K_{R2}	P^*	K_{R2}	P^*
0·0	4·046	1·6	5·172	6·0	6·631	24·0	7·865
0·4	4·380	2·0	5·381	10·0	7·186	30·0	7·981
0·8	4·676	3·0	5·813	14·0	7·492	50·0	8·178
1·2	4·938	4·0	6·149	18·0	7·683	∞	8·502

TABLE 5

Buckling loads for plate with elastic support along one edge ($\phi = 1/2{\cdot}5$)

K_{R2}	P^*	K_{R2}	P^*	K_{R2}	P^*	K_{R2}	P^*
0·0	1·429	1·6	1·833	6·0	2·350	24·0	2·782
0·4	1·549	2·0	1·907	10·0	2·545	30·0	2·823
0·8	1·655	3·0	2·061	14·0	2·652	50·0	2·891
1·2	1·749	4·0	2·180	18·0	2·719	∞	3·004

TABLE 6

Buckling loads for plate with equal elastic support along opposite edges ($K_{R2} = K_{R4}$, $\phi = 1{\cdot}0$)

K_{R2}	P^*	K_{R2}	P^*	K_{R2}	P^*	K_{R2}	P^*
0·0	9·276	1·6	14·74	6·0	23·44	24·0	32·86
0·4	10·81	2·0	15·85	10·0	27·42	30·0	33·85
0·8	12·23	3·0	18·29	14·0	29·79	50·0	35·57
1·2	13·53	4·0	20·31	18·0	31·34	∞	38·45

elastic support along one edge only, and the fixed in-plane loading, denoted by the symbol P_{REFF}, is set equal to 80% of the buckling load of a similar plate with no rotational elastic support along either edge. The choice of in-plane loading is strictly arbitrary. It permits us to plot data for a typical plate loading and set of

TABLE 7

Buckling loads for plate with equal elastic support along opposite edges ($K_{R1} = K_{R4}$, $\phi = 1{\cdot}5$)

K_{R2}	P^*	K_{R2}	P^*	K_{R2}	P^*	K_{R2}	P^*
0·0	21·23	1·6	33·54	6·0	53·16	24·0	74·49
0·4	24·69	2·0	36·04	10·0	62·16	30·0	76·74
0·8	27·88	3·0	41·54	14·0	67·53	50·0	80·62
1·2	30·82	4·0	46·10	18·0	71·05	∞	87·15

TABLE 8

Buckling loads for plate with equal elastic support along opposite edges ($K_{R2} = K_{R4}$, $\phi = 2{\cdot}5$)

K_{R2}	P^*	K_{R2}	P^*	K_{R2}	P^*	K_{R2}	P^*
0·0	59·93	1·6	94·11	6·0	148·7	24·0	208·3
0·4	69·54	2·0	101·0	10·0	173·8	30·0	214·6
0·8	78·39	3·0	116·4	14·0	188·9	50·0	225·4
1·2	86·56	4·0	129·1	18·0	198·7	∞	243·7

TABLE 9

Buckling loads for plate with equal elastic support along opposite edges ($K_{R2} = K_{R4}$, $\phi = 1/1{\cdot}5$)

K_{R2}	P^*	K_{R2}	P^*	K_{R2}	P^*	K_{R2}	P^*
0·0	4·046	1·6	6·472	6·0	10·32	24·0	14·47
0·4	4·728	2·0	6·966	10·0	12·08	30·0	14·91
0·8	5·357	3·0	8·045	14·0	13·12	50·0	15·66
1·2	5·937	4·0	8·940	18·0	13·81	∞	16·93

TABLE 10

Buckling loads for plate with equal elastic support along opposite edges ($K_{R2} = K_{R4}$, $\phi = 1/2{\cdot}5$)

K_{R2}	P^*	K_{R2}	P^*	K_{R2}	P^*	K_{R2}	P^*
0·0	1·429	1·6	2·301	6·0	3·675	24·0	5·141
0·4	1·675	2·0	2·478	10·0	4·297	30·0	5·294
0·8	1·901	3·0	2·864	14·0	4·666	50·0	5·558
1·2	2·109	4·0	3·183	18·0	4·906	∞	6·005

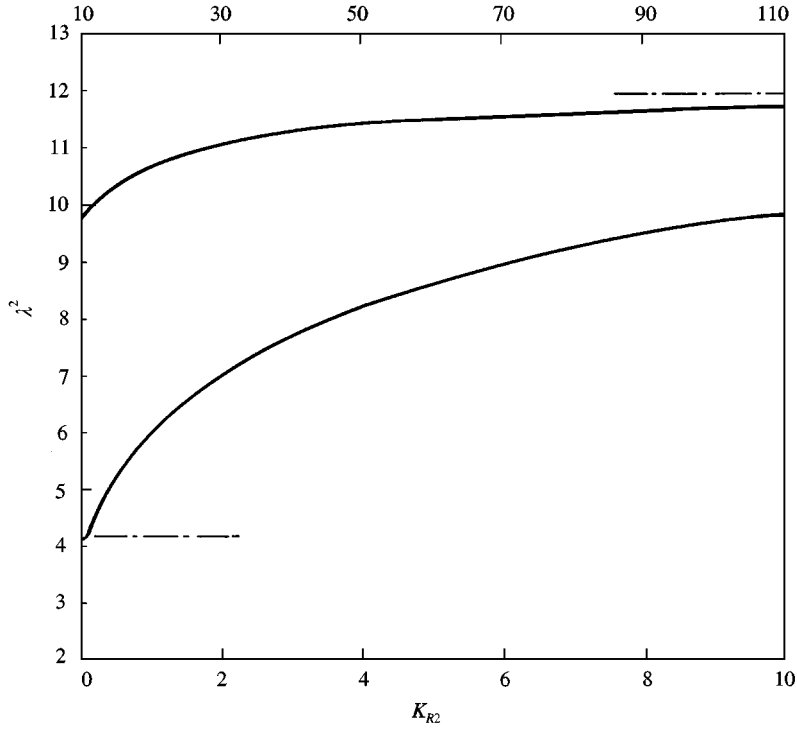

Figure 5. First mode free vibration eigenvalue versus rotational elastic edge stiffness for square plate with elastic support along one edge, only; $P_\xi = P_{REFF}$.

boundary conditions. A comparison plot for the same plate with the same in-plane loading, but equal rotational elastic support at opposite edges, is presented in Figure 6.

Again it is seen that sensitivity of the eigenvalue curves to changes in the elastic stiffness coefficient is much higher at the beginning of the range of this latter parameter.

Tabulated eigenvalues for the first four free vibration modes of the above plates are presented in Tables 10 and 11 respectively. Intervals in the elastic stiffness coefficient are the same as those utilized earlier in tabulation of buckling loads. All these results were obtained by initially plotting eigenvalue versus stiffness curves of the type shown in Figures 3 and 4. In this way it is verified that continuous curves are obtained in each case, beginning at the correct limit and approaching the correct limit as elastic stiffness is increased. This procedure helps to verify that no eigenvalues are missing.

4. SUMMARY AND CONCLUSIONS

It is found that the superposition method as exploited here is ideally suited for establishing accurate buckling loads, as well as free vibration frequencies and mode shapes, for plates with two opposite edges free and uniform compressive or tensile

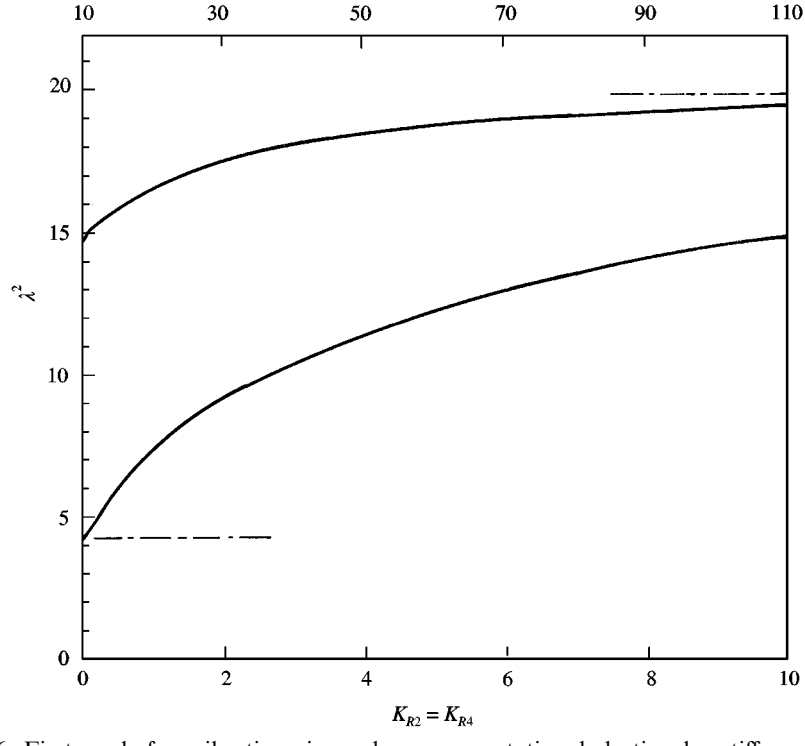

Figure 6. First mode free vibration eigenvalue versus rotational elastic edge stiffness for square plate with equal elastic support along opposite edges; $P_\xi = P_{REFF}$.

TABLE 11

First four eigenvalues, λ^2, for square plate with elastic support on one edge only; K_{2R} as indicated ($P_\xi = P_{REFF}$)

	Mode			
K_{R2}	1	2	3	4
0·0	4·279	13·38	34·81	35·40
0·4	5·075	13·66	35·25	35·51
0·8	5·692	13·91	35·61	35·66
1·2	6·192	14·13	35·70	36·04
1·6	6·611	14·33	35·79	36·40
2·0	6·969	14·51	35·87	36·73
3·0	7·674	14·90	36·06	37·47
4·0	8·198	15·21	36·22	38·11
6·0	8·931	15·69	36·48	39·15
10·0	9·775	16·29	36·85	40·58
14·0	10·25	16·66	37·10	41·53
18·0	10·55	16·91	37·28	42·19
24·0	10·85	17·16	37·48	42·89
30·0	11·04	17·32	37·61	43·37
50·0	11·37	17·62	37·87	44·25
∞	11·94	18·17	38·39	45·95

TABLE 12

First four eigenvalues, λ^2, for square plate with elastic support on opposite edges; ($K_{R2} = K_{R4}$); K_{2R} as indicated ($P_\xi = P_{REFF}$)

	Mode			
K_{R2}	1	2	3	4
0·0	4·279	13·38	34·81	35·40
0·4	5·787	13·94	35·69	35·62
0·8	6·893	14·44	35·82	36·49
1·2	7·780	14·89	36·01	37·24
1·6	8·522	15·30	36·19	37·94
2·0	9·160	15·67	36·36	38·59
3·0	10·44	16·48	36·75	40·04
4·0	11·42	17·15	37·09	41·30
6·0	12·84	18·19	37·65	43·34
10·0	14·59	19·57	38·49	46·22
14·0	15·64	20·45	39·06	48·17
18·0	16·33	21·05	39·49	49·57
24·0	17·04	21·68	39·95	51·06
30·0	17·51	22·11	40·28	52·11
50·0	18·36	22·90	40·93	54·11
∞	19·92	24·41	42·29	58·16

in-plane loading applied normal to the other two edges. Lateral displacement is forbidden along the in-plane loaded edges and these edges may be given any desired level of rotational elastic stiffness.

Convergence is rapid and results computed to four significant digit accuracy are easily achieved. The reader will agree, as pointed out earlier, that only a small portion of possible combinations of in-plane loading and elastic edge support stiffness can be investigated here. The results presented permit one to gain some insight into the variation of buckling loads and free vibration frequencies, with elastic stiffness coefficients. Of equal or perhaps greater value, is the fact that these plotted and tabulated results provide other researchers with accurate data against which their findings may be compared. It will also be obvious that the analytical procedure described here can be extended to handle the analysis of plates with other combinations of plate elastic edge support combined with uni-directional, or bi-directional, in-plane loading.

REFERENCES

1. D. J. MICHELUSSI, 1996 *M.Sc. Thesis, Department of Mech. Eng., University of Ottawa.* Free vibration and buckling analysis of thin rectangular plates with classical boundary conditions under unilateral in-plane loads.
2. S. D. YU and D. J. GORMAN 1990 *Proceedings of the Canadian Society for Mechanical Engineering, Mechanical Engineering Forum*, Vol. IV, 121, 126. Free vibration of fully clamped rectangular plates subjected to constant in-plane loads.

3. W. L. Cleghorn and S. D. Yu 1992 *Transactions of the Canadian Society of Mechanical Engineering* **16**, 185–199. Analysis of buckling of rectangular plates using the method of superposition.

APPENDIX A: NOMENCLATURE

a, b	rectangular plate edge lengths
D	plate flexural rigidity $= Eh^3/12\,(1 - \nu^2)$
E	modulus of elasticity of plate material
h	plate thickness
k	basic rotational elastic stiffness coefficient
K_R	dimensionless rotational stiffness $= ka/D$
M	bending moment.
$\frac{Mb^2}{aD}, \frac{Ma}{D}$	dimensionless bending moments associated with η and ξ directions respectively
P_x	in-plane compressive loading per unit length along the plate edge
P_ξ	dimensionless in-plane edge loading $= P_x b/D$
P_{REFF}	80% of dimensionless in-plane buckling load for square plate with zero elastic support along the opposite edges
V	plate vertical edge reaction
$\frac{Vb^3}{aD}$	dimensionless vertical edge reaction associated with η direction
w	plate lateral deflection as a function of x, and y
W	plate lateral displacement divided by edge length a, as a function of ξ and η
x, y	rectangular plate co-ordinates
ξ, η	$= x/a$, and $= y/b$ respectively
ϕ	plate aspect ratio, b/a
ν	Poisson ratio of plate material
ν^*	$= 2 - \nu$
λ^2	free vibration eigenvalue $= \omega a^2 \sqrt{\rho/D}$
ω	circular frequency of plate vibration
ρ	mass of plate per unit area